

Fluorescent Lighting Distribution for Plant Micropropagation

Chiachung Chen

Department of Bio-industrial Mechatronics Engineering, National ChungHsing University, 250 Kuokuang Road, Taichung 40227, Taiwan; e-mail: ccchen@dragon.nchu.edu.tw

(Received 24 March 2004; accepted in revised form 18 October 2004; published online 25 January 2005)

The cloning of plants can be produced in culture vessels by a micropropagation technique. It is popular to produce genetically uniform plantlets for the plant production industry to enhance profitability. Many culture vessels were placed on the shelves and many sets of successive horizontal shelves were arranged in the culture room. The fluorescent tubes installed above the vessels provided the light source for the culture vessels. The distribution uniformity of the lighting systems was very important for maintaining the quantity of plantlets. The model of lighting distribution for plant micropropagation was developed in this study. The photon flux density at different locations under various mounting heights and positions for the luminaries were measured at a full scale of the micropropagation shelf. The fitting agreements of three models were evaluated, including the line model, ribbon model, and empirical regression models. The ribbon model had the best fitting ability. The effect of height and spacing of fluorescent tubes on the distribution uniformity of light photon flux density was evaluated by the sensitivity analysis.

© 2004 Silsoe Research Institute. All rights reserved
Published by Elsevier Ltd

1. Introduction

Agricultural biotechnology has become the dominant industry in Taiwan. The orchid industry has developed so rapidly that the requirement of tissue culture plantlets has increased. To ensure the quality and quantity of plantlets, the growth environment of plantlets must be kept at the optimum condition.

Tissue culture plantlets *in vitro* are cultured in a small closed system of culture vessels. Many sets of successive horizontal shelves are arranged in the culture room, and many vessels are placed on the shelves. The important environmental factors affecting the growth of plantlets included light irradiance, air temperature, relative humidity, and carbon dioxide (CO₂) concentration (Aitken-Chrisie *et al.*, 1994). The way to modify the internal microclimate of vessels is to adjust the outside environment of culture room indirectly. The effect of the external condition on the internal climate of culture vessel, such as temperature and relative humidity, has been studied (Chen & Chen, 2002; Chen, 2003, 2004).

The irradiance on the culture vessel was called the photon flux density (Fujiwara & Kozai, 1995; Ciolkosz

et al., 1996). The wavelength values ranging from 400 to 700 nm were considered for the requirement of tissue culture plantlets. The unit of the photon flux density is $\mu\text{mol m}^{-2} \text{s}^{-1}$. The long-tube type of fluorescent lamps usually served as the light source to provide a horizontal distribution of photon flux density on culture shelves. Fujiwara and Kozai (1995) mentioned the factors affecting the photon flux density: the type and number of the light sources, the position of the vessel on the culture shelf, the position of the light sources, the optical characteristics of the shelf, and the materials and the shape of culture vessels.

The cost of lighting systems is very important for a micropropagation factory. According to the survey of Standaert de Metsenaere (1991), electricity accounts for 5–6% of the total costs. The two major constituents of this cost are lighting of the shelves for the vessels in the culture room (65%) and cooling of the culture room (25%). To increase the space utilisation of culture rooms, more shelves were installed. As the mounted heights decreased, more shelves could be installed and the space use efficiency of shelves was increased. However, the reduction in mounting heights caused a

| | | Notation | |
|-------------------------------------|---|-----------|---|
| b_0, b_1, b_2, b_3 , coefficients | | L_2 | the first fluorescent tube length of the right side, m |
| b_4, b_5, b_6 | | | |
| c_0, c_1, c_2, c_3 , coefficients | | L_3 | the second fluorescent tube length of the left side, m |
| c_4, c_5, c_6 , | | | |
| c_7, c_8, c_9 , | | L_4 | the second fluorescent tube length of the right side, m |
| c_{10}, c_{11} | | | |
| dE_n | units of the irradiance photon flux density normal to the line source, $\mu\text{mol m}^{-3} \text{s}^{-1}$ | n | number of data |
| | | R^2 | coefficient of determination |
| | | r | distance between the unit source and the measured point, m |
| dl | unit length of the fluorescent tube, m | S | length of AP, m |
| D_{MR} | mean relative deviation | s | standard errors of estimated values |
| d_1 | longitudinal distance between the point Q and the measurement point P, m | X_i | predicted light photon flux densities by lighting model, $\mu\text{mol m}^{-2} \text{s}^{-1}$ |
| d_2 | longitudinal distance between the point R and the measurement point P, m | Y_{ave} | average of measured light photon flux density, $\mu\text{mol m}^{-2} \text{s}^{-1}$ |
| E_n | total irradiance photon flux density normal to the line source, $\mu\text{mol m}^{-2} \text{s}^{-1}$ | Y_i | actual measured photon flux density, $\mu\text{mol m}^{-2} \text{s}^{-1}$ |
| E_{v1} | photon flux density from the left-hand side of fluorescent tubes, $\mu\text{mol m}^{-2} \text{s}^{-1}$ | y_1 | distance of the first fluorescent tube from the edge of the shelf, m |
| E_{v2} | photon flux density from the right-hand side of fluorescent tubes, $\mu\text{mol m}^{-2} \text{s}^{-1}$ | y_2 | lamp spacing, m |
| E_{vt} | photon flux density from the fluorescent tubes, $\mu\text{mol m}^{-2} \text{s}^{-1}$ | y_3 | distance of the second fluorescent tube from the edge of the shelf, m |
| e_i | predicted errors, $\mu\text{mol m}^{-2} \text{s}^{-1}$ | Z_i | distance between the lip of culture vessel and the edge of the shelf, m |
| e_{PR} | predictive performance, $\mu\text{mol m}^{-2} \text{s}^{-1}$ | $ P_i $ | absolute value of predictive errors, $\mu\text{mol m}^{-2} \text{s}^{-1}$ |
| e_{RMA} | relative mean absolute error | β | angle between AQ and AP, deg |
| H | height of light source, m | μ | angle between AP and BP, deg |
| I | irradiance flux from the fluorescent tube, W m^{-2} | μ_0 | angle between PA and PC, deg |
| K | conversion constant, $\mu\text{mol W}^{-1} \text{s}^{-1}$ | θ | angle between BP and BM, deg |
| L_1 | the first fluorescent tube length of the left side, m | | |

decrease in the uniformity of useful light reaching the plantlets. The best compromise between space efficiency and uniformity of illumination required investigation.

Fujiwara *et al.* (1989) investigated the effects of closures and test tube vessels on light density distribution. They found four different types of closure (aluminium foil cap, translucent polypropylene formed cap, silicon foam rubber plug, and transparent polycarbonate formed lid) all reduced the light transmittance.

Kitaya *et al.* (1995) observed the effects of light density and direction on the photoautotrophic growth and morphology of potato plantlets *in vitro*. The shoot length was shorter in the sideward lighting treatment than in the downward lighting treatment at different photon flux density levels. However, the dry weights,

fresh weights and leaf area of the plantlets revealed no significant difference in the two different light directions. These growth characteristics increased with increasing light level to $90 \mu\text{mol m}^{-2} \text{s}^{-1}$ and then decreased.

Ciolkosz *et al.* (1996) evaluated five models of fluorescent lighting systems for micropropagation. These techniques were: (1) the regression empirical model; (2) the point source model; (3) the lumen model; (4) the integrated area Fourier series (IAFS) model; and (5) the application distance photometry (ADP) model. They found that the IAFS model was the best one to calculate the average photon flux density at the vessel lid level. The regression empirical model was the adequate model for the average photon flux density at the plant level. The result of this study was adopted to serve as a design issue for micropropagation lighting systems

(Ciolkosz *et al.*, 1997). After comparing the measured photon flux density at different vessel conditions, Ciolkosz *et al.* (1997) found that the agar and plant material in the vessels had only little effect on the photon flux density at the vessel lid. Measurements at the plant level with or without agar and plantlets indicated the same trends. The IAFS model was developed by the assumption that the luminous intensity distribution of the luminaire was homogeneous across its luminous length and was proportional to the far-field photometric distribution. However, as the far-field techniques are used for near-field situations, the predicted errors were in the range of 20–40% (Ngai, 1993).

Economou and Read (1987) reported the optimum levels of photon flux density for some species. Walker *et al.* (1991) found that the growth rates of sugarcane plantlets increased with the increase of photon flux density. Spectral quality of light had significant effects on the plantlets (Dooley, 1991). However, these reports were varied and some growth characteristics were conflicting. Lees (1994) found that increased light level *in vitro* may increase the quality of some plantlets and decreased the growth quality of some species.

In order to obtain even distribution of photon flux density on culture vessels, the arrangement of the light sources is very important. The fluorescent lamps was the type of widely available long-tube light source, and so was adopted to provide horizontal uniformity distribution of photon flux density for all the culture vessels on the shelf. The mounting height and installation distance of fluorescent lamps had significant effects on the quantity and uniformity of photon flux density. The photon flux density distribution of vessel needs to be studied to quantify the effects of factors on the culture vessels.

2. Materials and methods

2.1. Culture vessel

A conical flask (F-1, I-Shin Co., Taiwan) was selected to measure the photon flux density at the lip level and at the plantlet level. The sketch of this vessel has been described elsewhere (Chen, 2003). The height of this vessel was 0.15 m and the diameter of the base was 0.10 m.

2.2. Light photon flux density measuring equipment

Light photon flux density in $\mu\text{mol m}^{-2} \text{s}^{-1}$ from fluorescence lamps was measured by LI-190SA quantum

Sensor (Li-COR Co., USA). This sensor was calibrated by Li-COR 1800-02 Optical Radiation Calibrator (Li-COR Co., USA). The accuracy of the meter was $\pm 3\%$ after calibrating (Fig. 1).

2.3. Experimental arrangement

A full scale micropropagation shelf was constructed. The layout of this shelf is shown in Fig. 2. The fluorescent tube spacing, mounting height, and vessel position can be adjusted. A single shelf, 0.9 m by 1.30 m, with two fluorescent luminaires mounted to the underside of an identical shelf. The length of fluorescent tubes, Philips TLD 36W/39, was 1.20 m. The space and the fixed positions of tubes could be adjusted according to the experimental design. The shelf held sixty conical flask vessels. This shelf was a standard unit for a tissue culture factory for the production of orchid plantlets.

The micropropagation shelf was placed in a culture room at the laboratory. The shelves were constructed of 0.03 m diameter steel pipe. All pipes and walls of the culture room were painted grey with 10% reflectance.

Before measurements were executed, the fluorescent tubes were turned for at least 1 h to stabilise the performance of the luminaires.

2.4. Measurement of light photon flux density

A LI-COR LI-190SA quantum sensor was applied to measure the light photon flux density. The measured positions included the vessel lid level and the plantlet level. The bottom of a special culture flask was removed carefully so that the sensor could be placed at the plantlet level [shown as Fig. 3(a)]. In order to observe the light distribution at the plantlet level, the measuring positions within the culture vessel were marked in the Fig. 3(b).

The photon flux densities at the two levels (vessel lid and plantlets) for different positions on the shelves were measured in the same way [Fig. 3(a)]. The transmittance was then calculated as the ratio of measurement values of that plantlet level and of the vessel lid level.

The measurement of the photon flux density of the lid level for culture vessels placed at various positions included the difference of the luminaire mounting heights and the spacing of the fluorescent tubes. All the calculated values by the three lighting models were compared with the actual measured values to evaluate the adequacy of these models. These light models are explained in the Appendix.

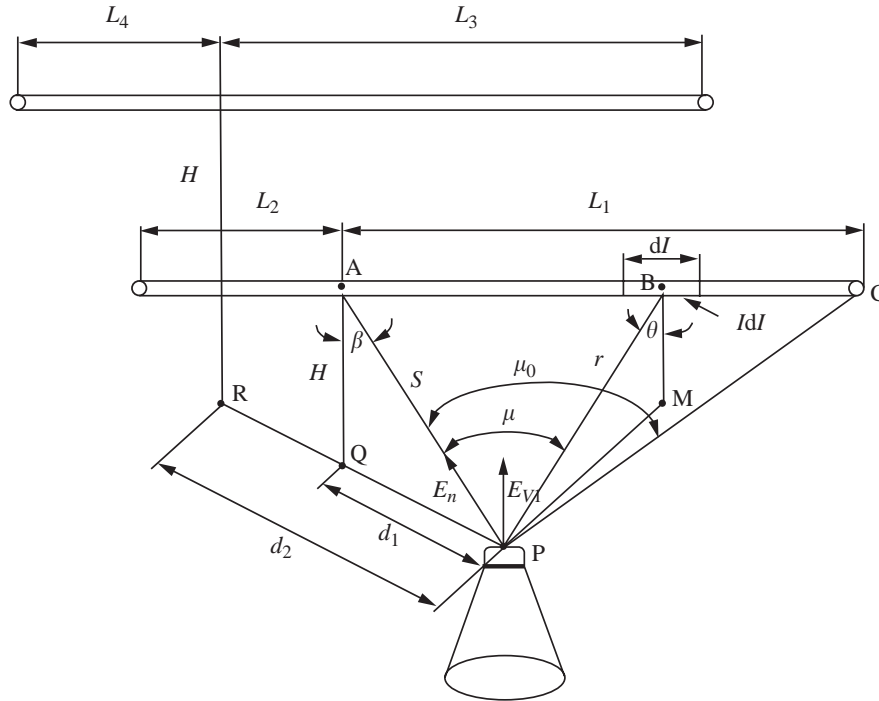


Fig. 1. Schematic diagram of the light photon flux density model: A is the fixed point for the AQ and QP has the vertical angle; B is the arbitrary point along the tube; dE_n , units of the irradiance photon flux density normal to the line source; dl , unit distance of fluorescent tube; d_1 , longitudinal distance between the point Q and the measurement point P; d_2 , longitudinal distance between the point R and the measurement point P; E_n , total irradiance photon flux density normal to the line source; E_{v1} , photon flux density from the left-hand side of fluorescent tubes; H , height of the light source; I , irradiance flux from the fluorescent; L_1 , the first fluorescent tube length of the left-hand side; L_2 , the first fluorescent tube length of the right-hand side; L_3 , the second fluorescent tube length of the left-hand side; L_4 , the second fluorescent tube length of the right-hand side; S , the distance between the height at point A and the measuring point P; β , angle between AQ and AP; μ , angle between AP and BP; μ_0 , angle between PA and PC; θ , angle between BP and BM

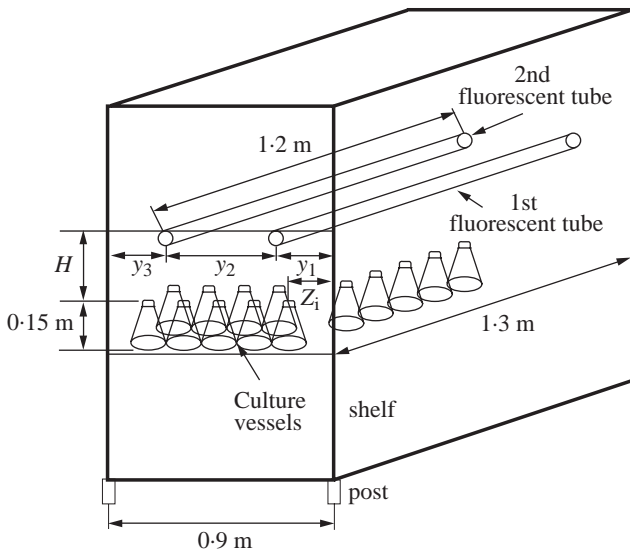


Fig. 2. General layout of culture vessel shelves; H , height of light source; y_1 , distance of the first fluorescent tube from the edge of the shelf; y_2 , lamp spacing; y_3 , distance of the second fluorescent tube from the edge of shelf; Z_1 , distance between the lip of culture vessel and the edge of the shelf

2.5. Data analysis

2.5.1. Evaluation of predictive performance

The quantitative criteria for the comparison of predictive performance were defined as follows.

(1) *Predictive errors*: The predictive errors e_i in $\mu\text{mol m}^{-2}\text{s}^{-1}$ of the i th measurement of photon flux density is given by

$$e_i = Y_i - X_i \tag{1}$$

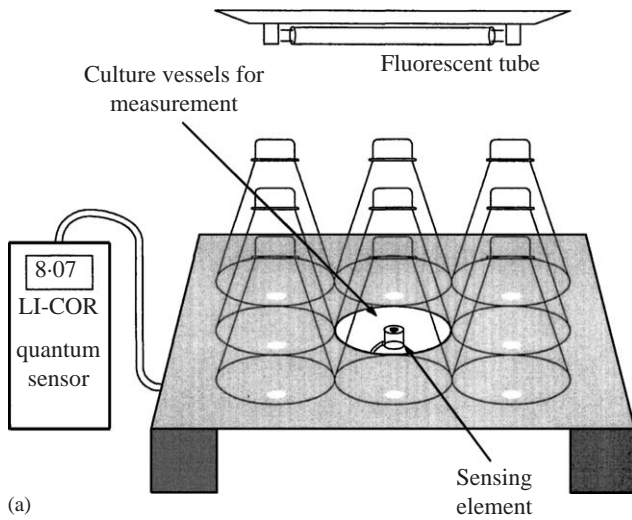
where: Y_i is the actual measured photon flux density in $\mu\text{mol m}^{-2}\text{s}^{-1}$; and X_i is the predicted light photon flux densities by lighting model in $\mu\text{mol m}^{-2}\text{s}^{-1}$.

(2) *Predictive performance*: The predictive error performance (PRE) denoted by e_{PR} in $\mu\text{mol m}^{-2}\text{s}^{-1}$ is

$$e_{PR} = \Sigma|e_i|/n \tag{2}$$

where: $|e_i|$ is the absolute value of predictive errors in $\mu\text{mol m}^{-2}\text{s}^{-1}$; and n is the number of data.

(3) *Relative mean absolute error*: The relative mean absolute error (RMAE) denoted by e_{RMA} in



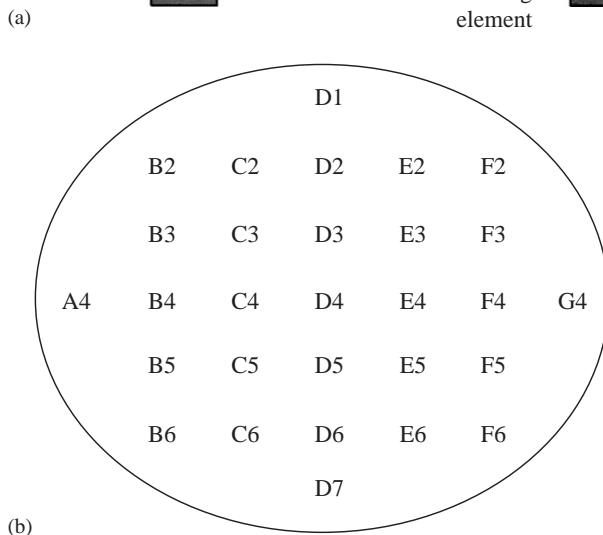
error e_i versus actual measured value Y_i was used to evaluate the predictive ability. As the residual plot reveals the uniform distribution pattern, this model can be considered to be an adequate model.

2.5.2. Evaluation of uniformity

The criterion of mean relative deviation D_{MR} for the evaluation of uniformity performance was defined as follows:

$$D_{MR} = \Sigma|(Y_{ave} - Y_i)/Y_{ave}|/n \quad (4)$$

where: Y_{ave} is the average of measured light photon flux density in $\mu\text{mol m}^{-2} \text{s}^{-1}$.



3. Results and discussion

3.1. The photon flux density distribution within culture vessel

The typical distribution of the transmittances within the culture vessel is presented in Fig. 3(c). The lower ratio values were found at boundary positions, such as the coordinates of A4, D1, D7, and G4. If the plantlets were transplanted in this position, the wall of culture vessels could retard growth. No plantlets were placed in this position in practical applications. These four numeric values were deleted for further analysis. The status of the transmittance data for the other 40 vessels was maximum value of 0.94, minimum value of 0.85, average value of 0.8944, standard deviation of 0.0249. These statistics indicated the good uniformity distribution of the light photon flux density in the vessel.

| | | | | | | | |
|---|------|------|------|------|------|------|------|
| | A | B | C | D | E | F | G |
| 1 | | | | 0.72 | | | |
| 2 | | 0.85 | 0.93 | 0.94 | 0.93 | 0.86 | |
| 3 | | 0.90 | 0.88 | 0.89 | 0.90 | 0.89 | |
| 4 | 0.80 | 0.89 | 0.92 | 0.92 | 0.93 | 0.90 | 0.78 |
| 5 | | 0.89 | 0.89 | 0.89 | 0.91 | 0.88 | |
| 6 | | 0.86 | 0.88 | 0.88 | 0.90 | 0.85 | |
| 7 | | | | 0.74 | | | |

3.2. The transmittance of culture vessels at various positions

In this measurement work, the height of two fluorescent tubes was 0.35m. Ninety culture vessels were arranged on the culture shelves. The measured point of internal photon flux density was located at the central position of the bases. The transmittance of these vessels versus the measured values of external photon flux density is shown in Fig. 4. At the higher measured values of the external photon flux density ranging from 50 to 70 $\mu\text{mol m}^{-2} \text{s}^{-1}$, the distribution of the transmittance was more scattering. However, no significant difference could be found by statistical analysis for the transmittance at different ranges.

$\mu\text{mol m}^{-2} \text{s}^{-1}$ is

$$e_{RMA} = \Sigma|P_i/Y_i|/n \quad (3)$$

The quality criterion for the comparison of predictive performance was the residual plot. The plot of predictive

Fig. 3. (a) Measurement of the internal transmittance of culture vessels placed on the shelf; (b) the measuring points for the internal transmittance for a unit vessel; and (c) internal transmittance distribution

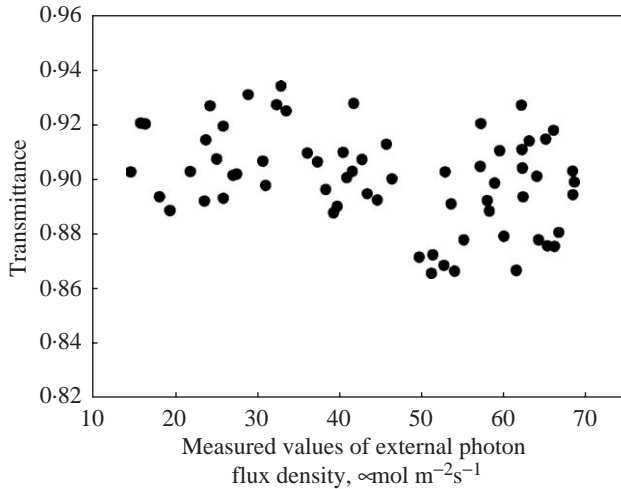


Fig. 4. Relationship between transmittance of these vessels and measured values of external photon flux density

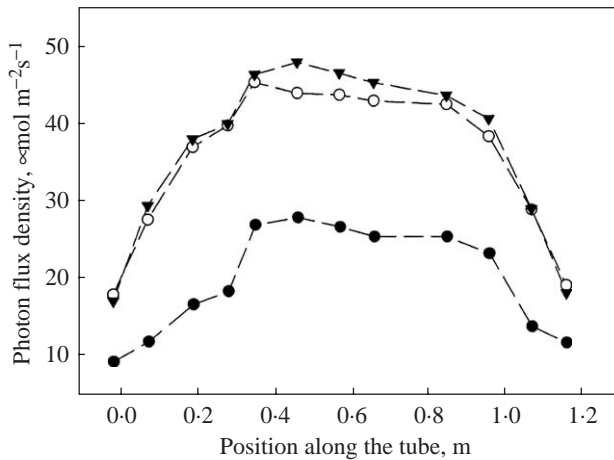


Fig. 5. Photon flux density distribution for vessels at the different distances Z_i between the lip of culture vessel and the edge of the shelf: \bullet , $Z_1 = 0.1\text{ m}$; \circ , $Z_2 = 0.3\text{ m}$; \blacktriangledown , $Z_3 = 0.4\text{ m}$

3.3. Evaluation of the lighting distribution model

In the first experiment, the height of fluorescent tube H was 0.3 m . The distance of the first fluorescent tube from the edge of the shelf y_1 was 0.22 m . The lamp spacing y_2 was 0.24 m .

The photon flux density at the different distances between the lip of the culture vessel and the edge of the shelf Z_i is shown in Fig. 5. The maximum photon flux density, $45.6\mu\text{mol m}^{-2}\text{s}^{-1}$, was located at the middle position. These values decreased quickly near both the lamp ends. The contour lines of photon flux density presented in Fig. 6 were drawn using the Sigma plots

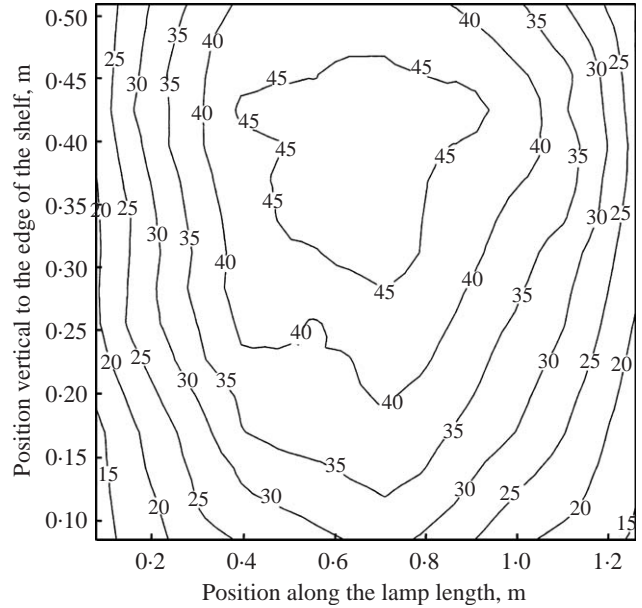


Fig. 6. Contour lines of photon flux density in $\mu\text{mol m}^{-2}\text{s}^{-1}$ for the first experiment

software version 8.0 (SPSS Inc., USA). The location of the maximum photon flux density was found in the central position along the length of the lamp and between two fluorescent lamps. The minimum values were located at both ends of the two fluorescent lamps and near the edge of the shelf. The distribution of the photon flux density indicated that the output of the fluorescent tube decreased along the length. At both the end positions, the minimum photon flux density was nearly $20\mu\text{mol m}^{-2}\text{s}^{-1}$. The average light photon flux density was $32.6\mu\text{mol m}^{-2}\text{s}^{-1}$. The mean relative deviation D_{MR} was 0.273 . The magnitude of light intensity decreased significantly on both sides. This condition has the critical effects on plantlets that are sensitive to the light quantity. From a practical viewpoint, the fluorescent tubes were arranged successively along the culture shelf. For the long shelf in the culture room, the light quantity on both sides of the fluorescent tubes needs to be considered.

If the data on photon flux density in Fig. 6 at both 5% edges of the tube length were deleted, the average photon flux density was $33.6\mu\text{mol m}^{-2}\text{s}^{-1}$ and the D_{MR} value was 0.212 . The uniformity of photon flux density was a significant improvement.

The predicted values of photon flux density calculated by the ribbon model were compared to the actual measured values. The contour line of predicted errors of photon flux density is presented in Fig. 7. No significant errors pattern could be found. The residual distribution of the ribbon model for this measurement is shown in Fig. 8. The predicted errors did not indicate any

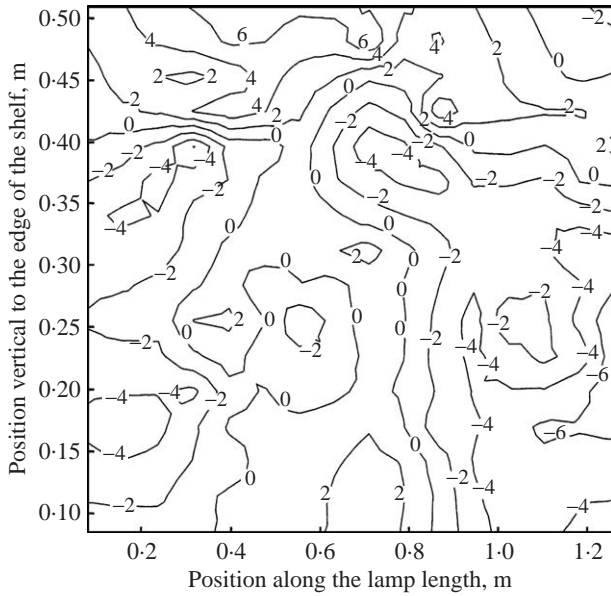


Fig. 7. Contour lines of predicted errors of photon flux density in $\mu\text{mol m}^{-2} \text{s}^{-1}$ for the first experiment

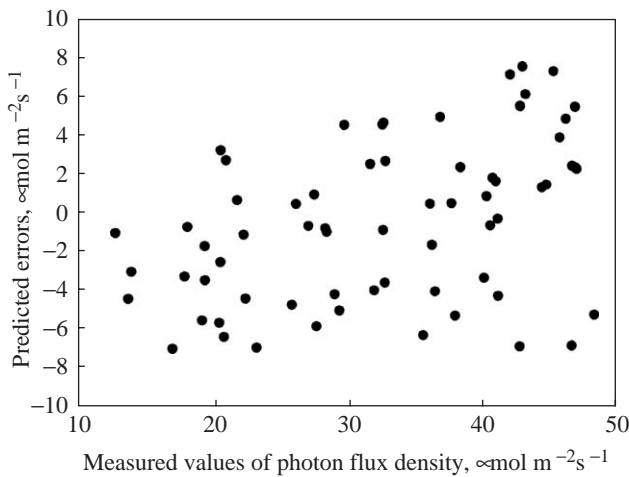


Fig. 8. Residual distribution of the ribbon model for the first measurement

significant pattern. The distribution of predicted errors and residual distribution of the line model for this measurement had similar results as in the ribbon model. Both models can be applied to predict the photon flux density distribution.

The e_{PR} value for this model was $4.82 \mu\text{mol m}^{-2} \text{s}^{-1}$ and the e_{RMA} value for the ribbon model was 0.161. The e_{PR} value for the model was $5.72 \mu\text{mol m}^{-2} \text{s}^{-1}$ and the e_{RMA} value for the line model was 0.195. Comparing e_{RMA} and e_{PR} values for both models, the quantitative predictive ability of the ribbon model was better than that of the line model.

The relationship between the actual measured photon flux density and other variables was established by regression analysis, the empirical equation being

$$E_n = 32.8 - 24.1d_1 - 51.23d_2 + 79.6L_1 - 67.4L_1^2 \quad (5)$$

with value for the coefficient of determination R^2 of 0.937, and standard deviation s of 2.673, where: E_n is the total irradiance photon flux density normal to the light source in $\mu\text{mol m}^{-2} \text{s}^{-1}$; d_1 is the distance between the vertical point for the first fluorescence tubes and measurement point in m; d_2 is the distance between the vertical point for the second fluorescence tubes and measurement point in m; and L_1 is the first fluorescent length of the left side in m.

The residual plots of Eqn (5) revealed a uniform distribution pattern. The predictive values of E_n from Eqn (5) were used to calculate the e_{PR} and e_{RMA} value. The e_{PR} value for this model was $4.04 \mu\text{mol m}^{-2} \text{s}^{-1}$ and the e_{RMA} value for the empirical model was 0.142. The quantitative criteria of the empirical model were better than those of the two theoretical models. However, the effect of mounting height of the fluorescent tubes was not considered in this empirical model.

In the second experiment, the mounting height H was kept at 0.3 m. The distance of the first fluorescent from the edge of shelf y_1 was 0.1 m. The lamp spacing y_2 was 0.24 m. The contour plot of light photon flux density is presented in Fig. 9. The maximum and minimum values of photon flux density were 45.2 and $20.1 \mu\text{mol m}^{-2} \text{s}^{-1}$, respectively. The predicted error by the ribbon model for this experiment is presented in Fig. 10. No clear

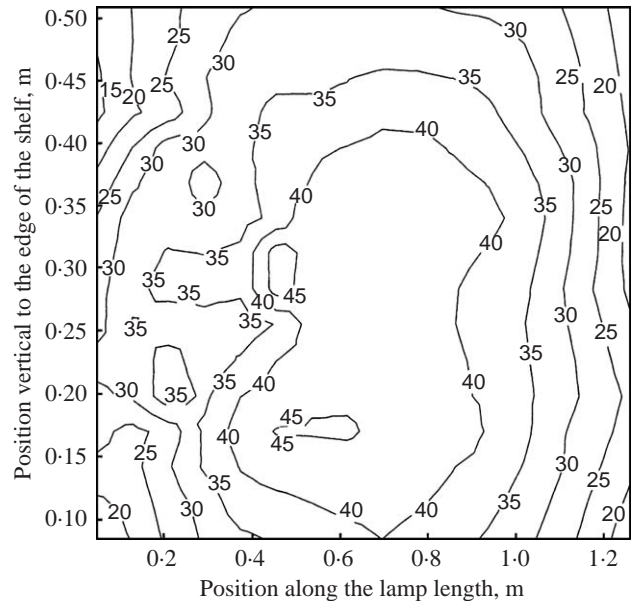


Fig. 9. Contour lines of photon flux density in $\mu\text{mol m}^{-2} \text{s}^{-1}$ for the second experiment

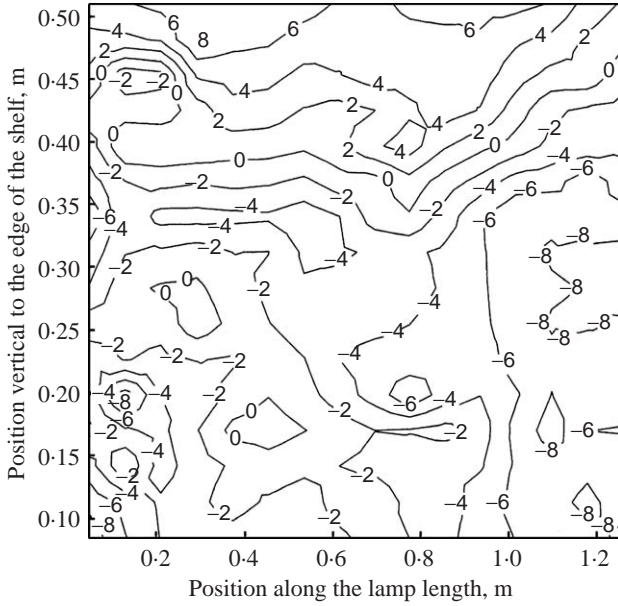


Fig. 10. Contour lines of predicted errors of photon flux density in $\mu\text{mol m}^{-2} \text{s}^{-1}$ for the second experiment

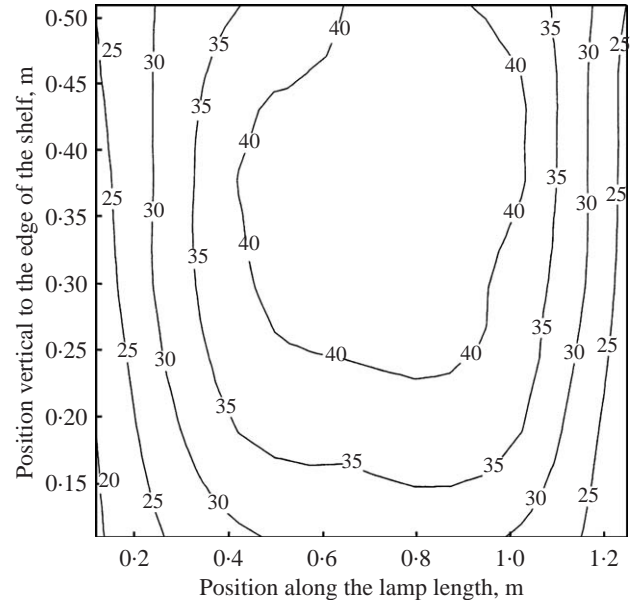


Fig. 11. Contour lines of photon flux density in $\mu\text{mol m}^{-2} \text{s}^{-1}$ for the third experiment

pattern of error distribution could be found. The residuals plot of the line model also indicated no clear pattern for the distribution of predictive errors. The average light photon flux density was $33.1 \mu\text{mol m}^{-2} \text{s}^{-1}$. The mean relative deviation D_{MR} is 0.2695.

The e_{PR} values for the ribbon model was $4.32 \mu\text{mol m}^{-2} \text{s}^{-1}$ and the e_{RMA} value for this model was 0.151. The e_{PR} value for the line model was $5.22 \mu\text{mol m}^{-2} \text{s}^{-1}$ and the e_{RMA} value for the model was 0.179. The ribbon model had the better predictive performance than that of the line model.

The empirical equation established by regression analysis for this experiment was

$$E_n = 28.9 - 20.9d_1 - 32.5d_2 + 71.9L_1 - 63.1L_1^2 \quad (6)$$

with value for the coefficient of determination R^2 of 0.924, and standard deviation s of 2.473.

The residual plots did not indicate any clear pattern. As the predicted values of E_n were computed from Eqn (6), the e_{PR} value and e_{RMA} value were calculated as $3.74 \mu\text{mol m}^{-2} \text{s}^{-1}$ and 0.142, respectively.

In the third investigation, the mounting height H was kept at 0.16 m. The distance of the first fluorescent tube from the edge of the shelf y_1 was 0.20 m. The lamp spacing y_2 was 0.24 m. The contour plot of measured results is shown in Fig. 11. The average light photon flux density was $32.5 \mu\text{mol m}^{-2} \text{s}^{-1}$ and the D_{MR} value was 0.413. As the height decreased, the scattering of lighting photon flux density was more obvious.

The e_{PR} value and the e_{RMA} value for the ribbon model was $5.44 \mu\text{mol m}^{-2} \text{s}^{-1}$ and 0.182. These values

for the line model were $6.29 \mu\text{mol m}^{-2} \text{s}^{-1}$ and 0.193. The residual plots all indicated their adequacy of the two models.

The empirical equation by regression analysis for this experiment was

$$E_n = -5.56 + 194.8d_1 - 30.74d_1^2 + 210.8d_2 - 63.63d_2^2 + 6019L_1 - 58.3L_1^2 \quad (7)$$

with the value of the coefficient of determination R^2 of 0.83, and standard deviation s of 3.91.

The e_{PR} value and e_{RMA} values calculated from the predicted E_n values were $5.94 \mu\text{mol m}^{-2} \text{s}^{-1}$ and 0.202, respectively.

Eqns (6)–(8) did not incorporate the term for the mounting height H . When all data from the three experiments were pooled, the pooled empirical equation was established as follows

$$E_n = 8.28 + 100.15d_1 - 131.18d_1^2 + 79.01d_2 - 175.59d_2^2 + 71.66L_1 - 62.18L_1^2 + 48.33H - 224.32d_1H - 169.78d_2H \quad (8)$$

with the value of the coefficient of determination R^2 of 0.71 and standard deviation s of 7.76.

The e_{PR} value and e_{RMA} values calculated from the predicted E_n values were $11.22 \mu\text{mol m}^{-2} \text{s}^{-1}$ and 0.532, respectively.

From the above result, the empirical model was an adequate model for the conditions of a fixed mounting height. When the variable of mounting height H was considered, the predictive ability of the empirical model

for photon flux density was not good enough. Comparing the quantitative criteria for e_{PR} and e_{RMA} , the ribbon model can serve as an adequate model to predict the distribution of light photon flux density for tissue culture vessels placed on the shelf.

3.4. Sensitivity analysis of model

To evaluate the effect of mounting height and spacing of the fluorescent tubes on the photon flux density distribution, a sensitivity analysis of the lighting distribution model was executed. The assumed conditions of the virtual shelf were as follows.

- (1) Only two fluorescent tubes were considered. The distance between the fluorescent tubes and edges of the shelf were identical systematically (that is, $y_1 = y_3$ in this case, where y_3 is the distance of the second fluorescent tube from the edge of shelf). This layout is a common case adopted by tissue culture factories for orchids plantlets.
- (2) The culture vessels were placed under three positions of shelf, L_1 values for each position were 0.30, 0.60 and 0.9 m, respectively.
- (3) The width of the shelf was 0.90 m. Twenty-nine culture vessels were placed below the fluorescent tubes.
- (4) The photon flux density was calculated by the ribbon model and then used to compare the uniformity performance.

The simulated result of average photon flux density is presented in Fig. 12. As the mounting height H increased, the average photon flux density decreased. Increasing the value of y_1 seems to provide a higher average photon flux density value. However, as y_1 values increased from 0.18 to 0.30 m, the increase of the average photon flux density was not significant. If the required light quantity of plantlets was assigned, the height of fluorescent tubes could be decided by this model.

From the data distribution, e_{RMA} values at different values for the height H and distance y_1 are presented in Fig. 13. Light density at the 0.20 m height had significant diversity. At the height of 0.4 m, the e_{RMA} values were the lowest of all compared to other treatments. This result indicated that the e_{RMA} value was reduced as the height H increased. Lower mounting heights of the fluorescent tubes would reduce the uniformity of light reaching the culture vessels. As the mounting heights of the fluorescent tubes increased, the photon flux densities reaching on the culture vessels were more uniform. The e_{RMA} values for the mounting heights of 0.35 and 0.4 m were most similar.

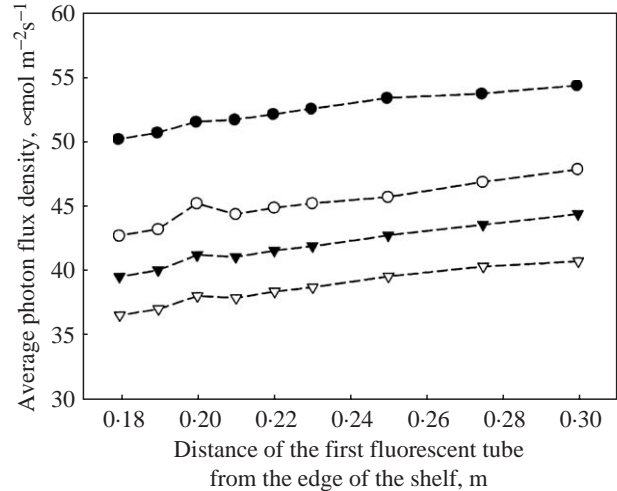


Fig. 12. Relationship between average photon flux density and distance of the first fluorescent tube from the edge of the shelf for different values of the fluorescent tube height H : ●, $H = 0.20$ m; ○, $H = 0.30$ m; ▼, $H = 0.35$ m; ▽, $H = 0.40$ m

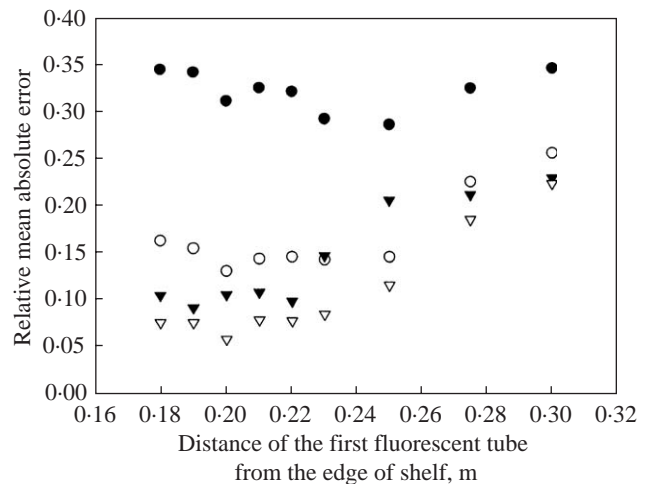


Fig. 13. Relationship between predictive performance and distance of the first fluorescent tube from the edge of the shelf for different values of the fluorescent tube height H : ●, $H = 0.20$ m; ○, $H = 0.30$ m; ▼, $H = 0.35$ m; ▽, $H = 0.40$ m

The effect of the tube position on the photon flux density also could be compared by the scattering data in Fig. 12. As the distance of the first fluorescent tube from the shelf edge y_1 was 0.3 m, the distance between two tubes y_2 was 0.4 m. The simulated results indicated that the e_{RMA} values at the condition of 0.2 m height was 0.35, and was 0.25, 0.24, and 0.23 for the y_1 values of 0.3, 0.35, and 0.40 m, respectively. As the y_1 values reduced, the distribution of e_{RMA} values became stable. At the y_1 value of 0.2 m, the e_{RMA} value was the lowest.

It indicated that the culture vessels have the most uniformity photon flux density in this treatment. The optimum conditions for the arrangement of fluorescent tubes was the distance of the first tube from the shelf y_1 was 0.2 m, and the distance between two tubes y_2 ranged from 0.35 to 0.40 m.

To maintain the optimum lighting photon flux density for the plantlets, an adequate lighting system is required. The factors affecting the photon flux density uniformity were the arrangement of the fluorescent tubes. The required light quantity was different for various plantlets. The ribbon model that was developed and validated in this study had the theoretical background and not only a form of pure empirical equation. The lighting distribution model could thus serve as a tool to help simulate the photon flux density distribution of a culture shelf and arrange the proper lighting system.

4. Conclusions

Three models of lighting distribution for plant micropropagation were developed in this study. The photon flux densities at different locations under various locations of the luminaries were measured at a full scale on the micropropagation shelf. The fitting agreements of three models were evaluated by comparing of measuring data and predicted values. The ribbon model had the best fitting ability. The effect of heights and spacing of the fluorescent tubes on the distribution uniformity of light flux intensity was evaluated by the sensitivity analysis. This lighting distribution model could thus serve as a tool to help simulate the photon flux density distribution of a culture shelf and arrange the proper lighting system.

Appendix A: light photon flux density model of culture shelves

Plant culture vessels are placed on shelves installed in the culture room. The fluorescent tubes were mounted to the underside of the other shelf above these vessels. A typical culture vessel for illuminating is sketched in *Fig. 1*. The light flux intensity on the lid of culture vessels can be derived by the lighting calculation method (Kisoh, 1997).

A1. The line model

The light source of fluorescent tube was assumed as a line source. The unit length of the fluorescent tube was dl . At the position P, the unit of the irradiance photon

flux density normal to the line source was dE_n and calculated as follows:

$$dE_n = (KI \cos^2 \mu dl)/r^2 \quad (A1)$$

where: dE_n is the units of the irradiance photon flux density normal to the line source in $\mu\text{mol m}^{-3} \text{s}^{-1}$; I is the irradiance flux from the fluorescent tube in W m^{-2} ; K is the conversion constant in $\mu\text{mol W}^{-1} \text{s}^{-1}$; dl is the unit length of fluorescent tube in m, r is the distance between the unit source and the measured point in m; and μ is the angle between AP and BP in degrees.

The total irradiance E_n can be found by integrating the dE_n value for all the length of tube:

$$E_n = \int_0^{L_1} dE_n \quad (A2)$$

where: L_1 is the length of the fluorescent tube of the left-hand side.

From the configuration of *Fig. 1*, $L_1 = S \tan \mu$, $dL_1 = S \sec^2 \mu d\mu$, and $r = S \sec \mu$, where: S is the length of AP in m; and μ is the angle between PA and PB in degree.

Eqn (A2) can be integrated as follows

$$\begin{aligned} E_n &= (KI/S) \int_0^{\mu_0} \cos^2 \mu d\mu \\ &= (KI/2S)(\mu_0 + \sin \mu_0 \cos \mu_0) \end{aligned} \quad (A3)$$

where: μ_0 is the angle between PA and PC in degree.

The vertical photon flux density can be calculated as follows:

$$E_{v1} = E_n \cos \beta \quad (A4)$$

where: E_{v1} is the vertical illumination from the left tube in $\mu\text{mol m}^{-2} \text{s}^{-1}$; and β is the angle between AQ and AP in degree.

From the configuration of *Fig. 1*,

$$\mu_0 = \tan^{-1}(L_1/S) \quad (A5)$$

$$S^2 = H^2 + d_1^2 \quad (A6)$$

where: H is the height of light source in m; and d_1 is the distance between the point Q and the measurement point P in m.

$$\sin \mu_0 = \frac{L_1}{\sqrt{S^2 + L_1^2}} \quad (A7)$$

$$\cos \mu_0 = \frac{S}{\sqrt{S^2 + L_1^2}} \quad (A8)$$

$$\cos \beta = \frac{H}{\sqrt{h^2 + d_1^2}} \quad (A9)$$

Combining Eqns (A4)–(A9), E_{v1} can be calculated as follows:

$$E_{v1} = \frac{KIH}{2\sqrt{H^2 + d_1^2}} \left\{ \frac{L_1}{H^2 + d_1^2 + L_1^2} + \frac{1}{\sqrt{H^2 + d_1^2}} \tan^{-1} \frac{L_1}{\sqrt{H^2 + d_1^2}} \right\} \quad (A10)$$

Thus, E_{v1} can be expressed as a function with the variables H , d_1 , and L_1 :

$$E_{v1} = f(H, d_1, L_1) \quad (A11)$$

The total irradiance photon flux density was the sum of irradiance from L_1 and L_2 tubes so the total irradiance photon flux density E_{vt} was calculated as follows

$$E_{vt} = E_{v1} + E_{v2} = f(H, d_1, L_1) + f(H, d_1, L_2) \quad (A12)$$

where: E_{v2} is the photon flux density from the right-hand side of fluorescent tubes in $\mu\text{mol m}^{-2} \text{s}^{-1}$; and L_2 is the fluorescent length of the right-hand side in m.

As two fluorescent tubes were applied, the height of two tubes was the same. The sum of light photon flux density can then be computed as follows

$$E_{vt} = f(H, d_1, L_1) + f(H, d_1, L_2) + f(H, d_2, L_3) + f(H, d_2, L_4) \quad (A13)$$

where: d_2 is the distance between the point R and the measurement point P; L_3 is the fluorescent length of the right-hand side for the second tube in m; and L_4 is the fluorescent length of the left-hand side for the second tube in m.

If two fluorescent tubes had different heights, the sum of light photon flux density can be computed by Eqn (A13) by substituting into different height H value.

A2. The ribbon model

The light source of the fluorescent tube was assumed as a ribbon source. The unit of the photon flux density dE_n can be calculated as follows

$$dE_n = (KI dl \cos \mu \cos \theta)/r^2 \quad (A14)$$

where: θ is the angle between BP and BM in degree; and r is the distance between the unit source and the measurement point P in m.

The irradiance E_n then be computed by integrating the dE_n value:

$$E_n = \int_0^{L_1} (KI \cos \theta \cos \mu dl)/r^2 \quad (A15)$$

From the configuration of Fig. 1,

$$\cos \theta = H/r = H \cos \mu/S \quad (A16)$$

Combining Eqns (A14) and (A16):

$$E_n = \frac{IKH}{2S^2} ((u_0 + \sin u_0 \cos u_0)) = \frac{IKH}{2S^2} \left\langle \frac{L_1 H}{S^2 + L_1^2} + \tan^{-1} \frac{L_1}{S} \right\rangle \quad (A17)$$

where: u_0 is the angle between PA and PC in degree.

The vertical photon flux density can be calculated as follows

$$E_{v1} = E_n \cos \beta = \frac{KIH^2}{2S^2 \left\langle \sqrt{H^2 + d_1^2} \right\rangle} \left[\frac{L_1 H}{H^2 + L_1^2} + \tan^{-1} \frac{L_1}{S} \right] \quad (A18)$$

Thus, E_{v1} can be expressed as a function of the variables h , d_1 , L_1 , S :

$$E_{v1} = g(H, d_1, L_1, S) \quad (A19)$$

The total irradiance E_{vt} was calculated as follows

$$E_{vt} = E_{v1} + E_{v2} = g(H, d_1, L_1, S) + g(H, d_1, L_2, S) \quad (A20)$$

As two fluorescent tubes were applied, the height of two tubes was the same. The sum of the light photon flux density then can be computed as follows

$$E_{vt} = g(H, d_1, L_1, S) + g(H, d_1, L_2, S) + g(H, d_2, L_3, S) + g(H, d_2, L_4, S) \quad (A21)$$

A3. The empirical equation

The empirical equation was not derived by the theoretical background. It was a pure polynomial form to express the relationship between E_n and other parameters.

A3.1. Model excluding the mounting height

At the fixed height, the empirical equation was

$$E_v = b_0 + b_1 d_1 + b_2 d_2 + b_3 L_1 + b_4 d_1^2 + b_5 d_2^2 + b_6 L_1^2 \quad (A22)$$

where: b_0 to b_6 are coefficients.

A3.2. Model included the mounting height

The empirical equation was

$$E_v = c_0 + c_1d_1 + c_2d_2 + c_3L_1 + c_4H + c_5d_1^2 + c_6d_2^2 + c_7L_1^2 + c_8H^2 + c_9d_1H + c_{10}d_2H + c_{11}L_1H \quad (\text{A23})$$

where: c_0 to c_{11} are coefficients.

References

- Aitken-Chrisie J; Kozai T; Smith M A L** (1994). Automation and Environmental Control in Plant Tissue Culture. Kluwer Academic Publishers, Dordrecht, The Netherlands
- Chen C** (2003). Development of a heat transfer model for plant tissue culture vessels. *Biosystems Engineering*, **85**(1), 67–77
- Chen C** (2004). Humidity in plant tissue culture vessels. *Biosystems Engineering*, **88**(2), 231–241
- Chen C; Chen J** (2002). Measurement of gas exchange rates for plant tissue culture vessels. *Plant, Cell, Tissue & Organ Culture*, **71**(2), 103–109
- Ciolkosz D E; Walke P N; Heinemann P H; Mistrick R G** (1997). Design issues for micropropagation lighting systems. *Transactions of the ASAE*, **40**(4), 1201–1206
- Ciolkosz D E; Walke P N; Mistrick R G; Heinemann P H** (1996). Modeling of fluorescent lighting systems for Micropropagation. *Transactions of the ASAE*, **39**(6), 2263–2269
- Dooley J H** (1991) Influence of lighting spectra on plant tissue culture. ASAE Paper No. 91-7530
- Economou A S; Read P E** (1987). Light treatments to improve efficiency on *in vitro* propagation systems. *HortScience*, **22**(5), 751–753
- Fujiwara K; Kozai T** (1995). Physical microenvironment and its effects. In: *Automation and Environmental Control in Plant Tissue Culture* (Aitken-Chistie J, ed), pp 319–369. Kluwer Academic Publishers, Dordrecht, The Netherlands
- Fujiwara K; Kozai T; Nakajo Y** (1989). Effects of closures and vessels on light intensities in plant tissue culture vessels. *Journal of Agricultural Meteorology*, **45**(3), 143–149
- Kisoh S** (1997). Lighting calculation. In: *Lighting Engineering* (The Japanese Lighting Society, ed), pp 79–101. Ohmsha Publishers, Tokyo, Japan
- Kitaya Y; Fukuda O; Kozai T; Kirdmanee C** (1995). Effects of light intensity and lighting direction on the photoautotrophic growth and morphology of potato plantlets *in vitro*. *Scientia Horticulturae*, **62**(1), 15–24
- Lees R P** (1994). Effects of the light environment on photosynthesis and growth *in vitro*. In: *Physiology, Growth, and Development of Plants in Culture* (Lumsden P J; Nicholas J R; Davies W J, eds), pp 31–46. Kluwer Academic Publishers, Dordrecht, The Netherlands
- Ngai P Y** (1993). On computation using far-field and near-field photometry. *Journal of the Illumine Engineering Society of North America*, **22**(2), 118–149
- Standaert de Metsenaere R E A** (1991). Economic considerations. In: *Micropropagation: Technology and Application* (Debergh P C; Zimmerman R H, eds), pp 123–140. Kluwer Academic Publishers, Dordrecht, The Netherlands
- Walker P N; Harris J P; Gautz L D** (1991). Optimal environment of sugarcane Micropropagation. *Transactions of the ASAE*, **34**(6), 2609–2614